

Laser flash photolysis study of bis(1,3-benzoxazol-2-yl) disulfide and bis(1,3-benzothiazol-2-yl) disulfide; reactivities of benzoxazol-2-ylsulfanyl and benzothiazol-2-ylsulfanyl radicals

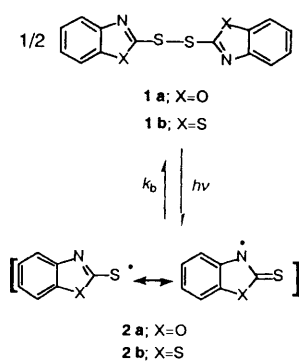
Maksudul M. Alam, Hideo Konami, Akira Watanabe and Osamu Ito*

Institute for Chemical Reaction Science, Tohoku University, Katahira, Aoba-ku, Sendai, 980-77, Japan

Photo-cleavage of the S–S bond of bis(1,3-benzoxazol-2-yl) disulfide and bis(1,3-benzothiazol-2-yl) disulfide have been studied by nanosecond laser flash photolysis. The transient absorption bands at *ca.* 590 nm were attributed to the radical species formed by S–S bond fission. Radical addition to conjugated dienes takes place forming the S–C bond, but not the N–C bond, as evidenced by the absence of the thione group in the product, suggesting that unpaired electron density is greater on the S atom of the primary radicals formed. From the decay rates of the radicals, the addition reaction rate constants for 2-methylbuta-1,3-diene are evaluated to be 3.0×10^8 and $5.0 \times 10^8 \text{ dm}^3 \text{ mol}^{-1} \text{ s}^{-1}$ in THF at 23 °C, respectively, for the benzoxazol-2-ylsulfanyl radical and the benzothiazol-2-ylsulfanyl radical. The reactivity of the latter radical is slightly higher than that of the former radical for all dienes studied. The low reactivity of these sulfanyl radicals with O₂, which is one of the characteristics of the S-centred radical, was confirmed. The rate constants for hydrogen abstraction from cyclohexa-1,4-diene are *ca.* $10^6 \text{ dm}^3 \text{ mol}^{-1} \text{ s}^{-1}$, which are *ca.* 1/100 compared with the addition reaction to conjugated dienes. MO calculations have been performed for these radicals to reveal the factors controlling the reactivity of the radicals.

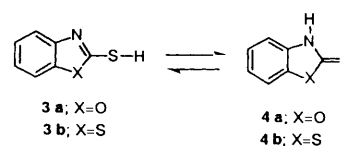
Bis(1,3-benzoxazol-2-yl) disulfide (**1a**) and bis(1,3-benzothiazol-2-yl) disulfide (**1b**) have been used as vulcanization accelerators of rubber; the key step of this complex procedure is presumed to be the formation of S-centred radicals from these disulfides.^{1,2} Recently, these disulfides have been used as efficient photo-initiators for vinyl polymerization.^{3,4} In the initiation of vinyl polymerization, it is important to study the photochemistry of these disulfides, elucidating the electronic structure and reactivities of the intermediate radicals. By applying Xe-flash photolysis, the reactivity of **2b** with various vinyl monomers was evaluated taking the irreversible addition process into consideration.⁵

As shown in the resonance structures of Scheme 1, the



unpaired electron of the radical **2** produced by the photo-cleavage of the S–S bond may localize on either the S or the N atom. In order to clarify the reactivity and electronic structures, we employed nanosecond laser flash photolysis, which is quite useful to follow fast reactions.^{6,7}

The thiols (**3**) of these radical moieties are known to be present as tautomer mixtures with thiones (**4**) as shown in Scheme 2;⁸ therefore, it is interesting to compare the electronic structure of radical **2** with the tautomerism of the parent hydrides, **3** and **4**. The kinetic behaviour of these radicals



affords useful information of the structures of the radicals, in addition to spectral information and product analysis.

From the molecular orbital (MO) calculations, useful information can be obtained; the parameters of the singly occupied molecular orbitals (SOMO), calculated by the MO method, may reveal the kind of electronic factor that controls the reactivities of the free radicals. Furthermore, we can expect to clarify the influence of O and S in the oxazole and thiazole moieties, respectively, on the reactivity.

Results and discussion

The transient absorption spectrum observed by the laser flash photolysis of **1a** in acetonitrile with 266 nm light shows a main band at 590 nm with a weaker band at a wavelength below 385 nm (Fig. 1). The absorption intensity of the 590 nm band decreases homogeneously with time, while the band at 385 nm does not decay at least within 4 μs, as shown in Fig. 1. As shown in the inserted decay curves in Fig. 1, the time profiles of each absorption maximum indicates that these two absorption bands are attributed to different species.

In order to assign the transient absorption bands, a disulfide **6a** having the benzoxazol-2-ylsulfanyl moiety and *p*-chlorophenylsulfanyl moiety was prepared by steady-light photolysis of a mixture of **1a** with bis(*p*-chlorophenyl)disulfide **5** as shown in Scheme 3. The *p*-chlorophenylsulfanyl moiety was selected as a partner because of its sharp transient absorption band at 510 nm^{9–12} where appreciable transient absorption of **1a** was not present.

From the laser flash photolysis of compound **6a**, two transient absorption bands were observed at 510 and 590 nm, as

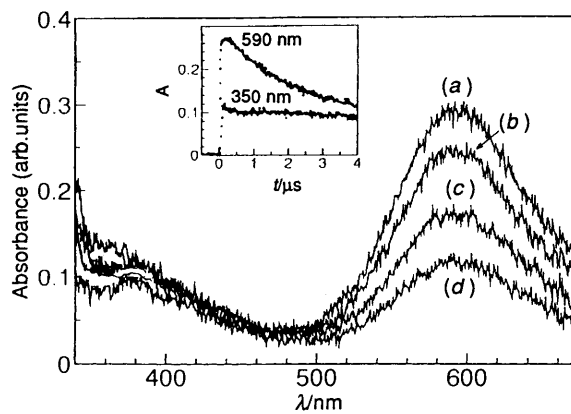


Fig. 1 Transient absorption spectra obtained by the laser photolysis (266 nm) of bis(1,3-benzoxazol-2-yl) disulfide **1a** ($1 \times 10^{-3} \text{ mol dm}^{-3}$) in acetonitrile in degassed solution; (a) 100, (b) 800, (c) 2000 and (d) 4000 ns. Insert: decay curves at 590 and 350 nm.

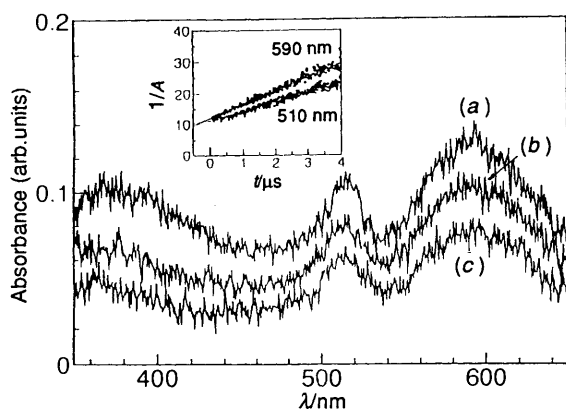
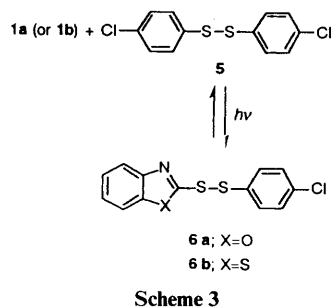
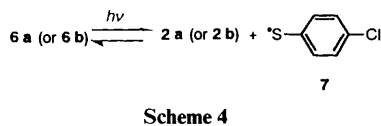


Fig. 2 Transient absorption spectra obtained by laser photolysis (266 nm) of disulfide **6a** ($0.5 \times 10^{-3} \text{ mol dm}^{-3}$) in THF. (a) 100, (b) 800 and (c) 2000 ns. Insert: second-order plots for the decays at 590 and 510 nm.

shown in Fig. 2. The transient absorption band at 510 nm was attributed to the *p*-chlorophenylsulfanyl radical (**7**).⁹⁻¹² Thus, this spectrum indicates that the photodissociation reaction occurs at the S-S bond, as shown in Scheme 4. Each absorption



intensity decays by second-order kinetics, suggesting that radicals **2** and **7** decay by radical coupling reactions to give disulfides **1**, **5** and **6**. At this stage, it is presumed that the transient absorption band at *ca.* 590 nm is attributed to the radical in which the unpaired electron density is largely on the S atom, because **2a** is common in Schemes 1 and 4. It is

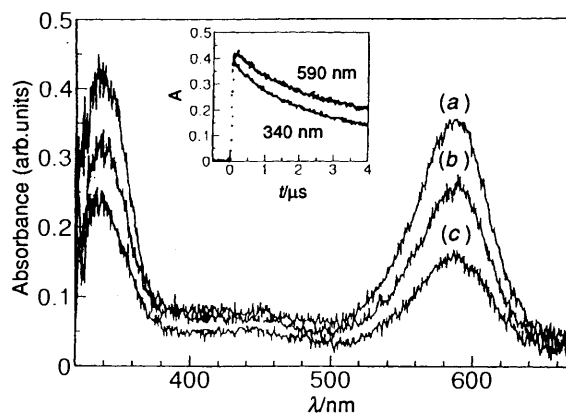


Fig. 3 Transient absorption spectra obtained by laser photolysis (266 nm) of bis(1,3-benzothiazol-2-yl) disulfide **1b** ($1 \times 10^{-3} \text{ mol dm}^{-3}$) in degassed acetonitrile. (a) 200, (b) 1000 and (c) 3000 ns. Insert: decay curves at 590 and 340 nm.

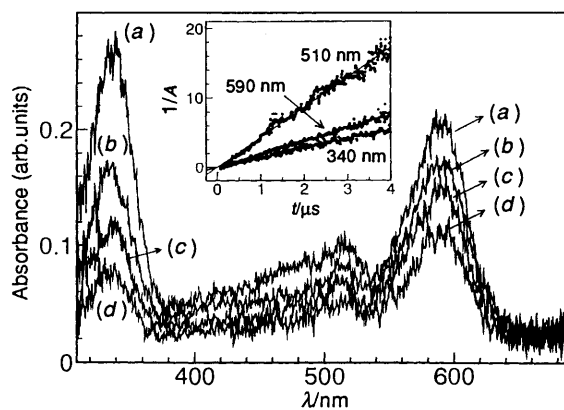


Fig. 4 Transient absorption spectra obtained by laser photolysis (266 nm) of disulfide **6b** ($1 \times 10^{-3} \text{ mol dm}^{-3}$) in acetonitrile. (a) 100, (b) 800, (c) 2000 and (d) 4000 ns. Insert: second-order plots for the decays at 340, 590 and 510 nm.

evident that disulfides **6**, are produced by the reaction at the S-centred radicals **2a** and **7** (Scheme 4).

In Fig. 1, the transient absorption band below 400 nm was quite stable within the timescale employed in this study (*ca.* 10 μs). Although this species was produced immediately after the laser pulse, the secondary species can be attributed to the prolonged absorption band; however, the 380 nm band could not be attributed to the thione **4a**, which has an absorption maximum at 320 nm. In less polar solvents, the other band tends to appear at *ca.* 450 nm. The decay rate of the species observed at 450 nm was also too slow to be observed by nanosecond laser photolysis.

In Fig. 3, the transient absorption spectra observed by the laser flash photolysis of **1b** are shown. The transient absorption band appears at 590 nm, which is in good agreement with the reported transient absorption band for **2b**, in which the unpaired electron localizes on the S atom.^{5,13} The band in the short wavelength region ($\lambda_{\text{max}} = 340 \text{ nm}$) decays at a similar rate to the 590 nm band. Thus, both bands at 590 and 340 nm in Fig. 3 were attributed to radical **2b**.¹⁴

Laser flash photolysis of **6b** led to transient absorption bands at 590, 510 and 340 nm as shown in Fig. 4. As the 510 nm band was attributed to radical **7**,⁹⁻¹² two sharp bands at 590 and 340 nm were attributed to radical **2b**, which may have S-centred radical character by analogy with **2a**.

By laser flash photolysis of **1b** in less polar solvents, a further absorption band appeared in the region of 400 and 500 nm. For example, in cyclohexane, an extra absorption band appears at 440 nm, which decays slowly, indicating a different species from radical **2b**.¹³

Table 1 The absorption maxima and second-order decay kinetics of 590 nm species (benzoxazol-2-ylsulfanyl radical **2a** and benzothiazol-2-ylsulfanyl radical **2b**)

Solvent	2a				2b		
	$k_d^a/10^9 \text{ mol dm}^{-3} \text{ s}^{-1}$	$\lambda_{\text{max}}/\text{nm}$	$(2k_b/\epsilon)/10^6 \text{ cm s}^{-1}$	$\epsilon^b/10^3 \text{ mol dm}^{-3} \text{ cm}^{-1}$	$\lambda_{\text{max}}/\text{nm}$	$(2k_b/\epsilon)/10^6 \text{ cm s}^{-1}$	$\epsilon^b/10^3 \text{ mol dm}^{-3} \text{ cm}^{-1}$
Hexane	21	575 ^b	25	17	570	2.0	20
Cyclohexane	6.8	575 ^b	1.7	8	573	1.1	12
Ethanol	5.6	590	1.3	8.6	587	1.2	9.3
THF	12	590	0.9	24	590	1.1	21
Acetonitrile	19	595	1.4	27	588	1.3	29

^a k_d is the diffusion controlled rate constant. ^b These ϵ values were evaluated from $2k_b/\epsilon$ assuming $k_b = k_d$.

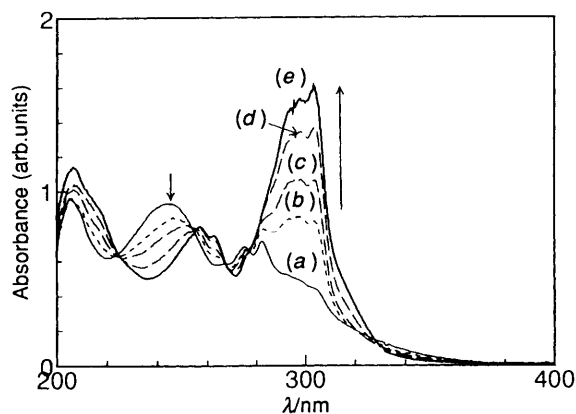


Fig. 5 UV spectral changes by steady-light photolysis of bis(1,3-benzoxazol-2-yl) disulfide ($0.1 \times 10^{-3} \text{ mol dm}^{-3}$) with Xe-lamp light longer than 270 nm in propan-2-ol in degassed solution; (a) 0, (b) 1, (c) 2, (d) 3 and (e) 7 min. Spectrum (e) is the same as spectrum of **4a**.

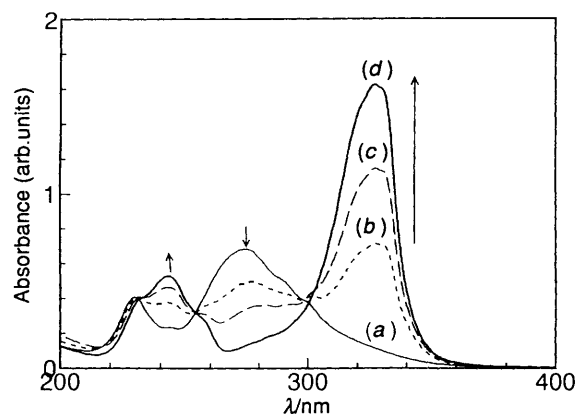
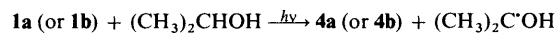


Fig. 6 UV spectral changes by steady-light photolysis of bis(1,3-benzothiazol-2-yl) disulfide **1b** ($0.1 \times 10^{-3} \text{ mol dm}^{-3}$) with Xe-lamp light longer than 270 nm in propan-2-ol in degassed solution; (a) 0 (b) 0.5, (c) 1 and (d) 3 min. Spectrum (d) is the same as spectrum of **4b**.

The transient bands at 590 nm in Figs. 1 and 3 decay with second-order kinetics, showing that the radicals decay mainly by recombination reaction to give the corresponding disulfides **1a** and **1b**. From the slope of the second-order plots, the ratios of the recombination rate constants (k_b) to the molar extinction coefficients (ϵ) were obtained. They are summarized in Table 1 for radicals **2a** and **2b** in various solvents with the longest wavelength absorption maximum (λ_{max}) of the radicals. Since the observed $2k_b/\epsilon$ values depend upon the viscosity (η) of the solvent, the recombination reaction may be close to the diffusion controlled limit (k_d). In tetrahydrofuran (THF), the k_d value is calculated to be $1.1 \times 10^{10} \text{ dm}^3 \text{ mol}^{-1} \text{ s}^{-1}$ from the Debye equation ($k_d = 8RT/3000\eta$).¹⁵ Thus, the ϵ value at 590 nm of **2a** was evaluated to be $ca. 24\,000 \text{ dm}^3 \text{ mol}^{-1} \text{ cm}^{-1}$, from which the initial concentration of **2a** from a laser exposure of disulfide **1a** is evaluated to be $ca. 0.01 \text{ mmol dm}^{-3}$ from the initial absorption intensity (Fig. 1). By one laser exposure of 1 mmol dm^{-3} disulfide **1a** solution, $ca. 1\%$ of the disulfide may be photo-cleaved under our experimental conditions. In most cases, the decay rate was not affected by addition of oxygen into the solution; thus, the reactivity of **2a** and **2b** with O_2 is low, which is characteristic of most arylsulfanyl radicals.¹⁶

In ethanol and cyclohexane, small ϵ values are estimated by the above method (Table 1). When the observed decay rate is faster than that anticipated from k_d , a small ϵ value would be evaluated. Thus, in ethanol and cyclohexane, some reaction may occur in addition to the radical coupling in keeping with second-order kinetics.

After photolysis of disulfide **1a** with steady light at $\lambda > 270$ nm (Xe-lamp) or with laser 266 nm pulsed light in propan-2-ol, new absorption bands appear at 308, 260 and 210 nm, which are attributed to thione **4a**, with the decrease in absorption intensity at 240 nm of disulfide **1a** (Fig. 5). The apparent reaction is shown in Scheme 5.

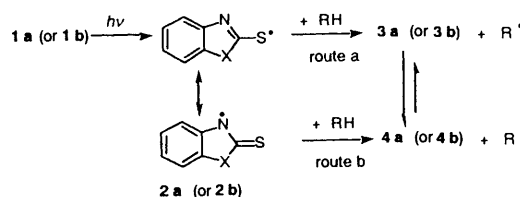


Scheme 5

Similarly, by photolysis of **1b** with steady light at $\lambda > 270$ nm (Xe-lamp) in propan-2-ol, new absorption bands appear at 330 and 245 nm which are attributed to thione **4b**, with a decrease in the absorption intensity at 270 nm of **1b** (Fig. 6).

In propan-2-ol, the decay time-profile of the 590 nm radical species shows two components; an initial fast decay and a later slow decay. The initial fast decay shows first-order kinetics with a rate constant of $7.0 \times 10^5 \text{ s}^{-1}$ for **2b**, from which the second-order rate constant for the hydrogen abstraction reaction of **2b** from propan-2-ol was evaluated to be $5.3 \times 10^4 \text{ dm}^3 \text{ mol}^{-1} \text{ s}^{-1}$.

Since the transient spectral data indicate that the unpaired electron density is localized mainly on the S atom of radicals **2a** and **2b**, our finding that the decay rates of the radicals are accelerated in propan-2-ol suggests that hydrogen abstraction takes place primarily at the S atom, thus forming thiols. Then, the appearance of the thione absorption in Figs. 5 and 6 may result from the tautomerism of thiols **3a** and **3b** into thiones **4a** and **4b**, respectively, as shown in route a in Scheme 6.



Scheme 6

Otherwise, it is also possible for the unpaired electron on the S atom is delocalized to the N atom in **2a** and **2b**, when the H

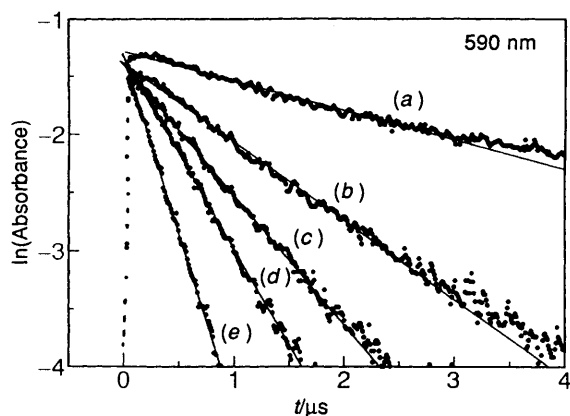


Fig. 7 First-order decay plots of the transient absorption intensity at 590 nm in the presence of 2-methylbuta-1,3-diene in deaerated THF solution; concentrations of 2-methylbuta-1,3-diene are (a) 0, (b) 1, (c) 2, (d) 4 and (e) 7×10^{-3} mol dm $^{-3}$

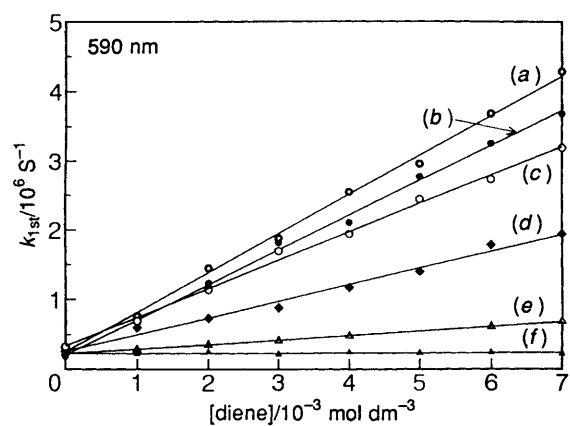


Fig. 8 Pseudo-first order plots (k_{1st} vs. [diene]) in THF; (a) 2,3-dimethylbuta-1,3-diene, (b) 2-methylbuta-1,3-diene, (c) 1,4-dimethylbuta-1,3-diene, (d) 1,1,4,4-tetramethylbuta-1,3-diene, (e) 1-methylbuta-1,3-diene and (f) cyclohexa-1,4-diene

atom of the hydrogen donor approaches the attacking radical as shown in route b in Scheme 6. At this stage, it is difficult to discriminate route a from route b.

By steady-light illumination of **1a** and **1b** in aerated propan-2-ol solution, the thione absorption bands due to **4a** and **4b** were almost suppressed. This suggests that radicals **2** may react with O₂, although the decay profiles of radicals **2** were not appreciably influenced by addition of O₂ in the timescale of 10 ns–10 μs in our laser flash photolysis method. Another possibility is that the photoreaction of thiol **3** by steady photoillumination takes place in the presence of O₂, resulting in the disappearance of **4**. In the case of 2-sulfanylpuridine, photo-induced oxidation of thiol has been found.¹⁷

On addition of 2-methylbuta-1,3-diene (isoprene), the decay rate of 590 nm band increases with the concentration of isoprene. In Fig. 7, the first-order plots of the decays are shown; a quite good linearity was observed. From the slopes of the lines, the first-order rate constants (k_{1st}) were evaluated.

The k_{1st} values thus observed have been plotted against the diene concentration as shown in Fig. 8. From the slope of the pseudo-first order plots, the second-order rate constants (k_a) were obtained. They are summarized in Table 2. The k_a values thus obtained in degassed solution are similar to those in aerated solution, suggesting that the addition reaction occurs irreversibly in the presence of excess diene in the timescale of a few μs employed in this study. In the case of **2b**, the k_a values obtained from the decay of the absorption band at 340 nm are in good agreement with those from the 590 nm band.

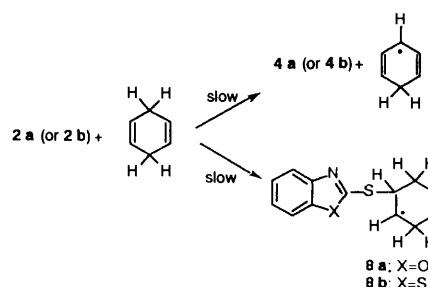
In the presence of cyclohexa-1,4-diene, which has four highly reactive hydrogens,^{18,19} the decay rates of **2a** and **2b** were only

Table 2 Rate constants (k_a) for reactions of **2a** and **2b** with various dienes at 23 °C in THF unless otherwise described

Diene	$k_a/10^8$ dm 3 mol $^{-1}$ s $^{-1}$ ^a	
	2a	2b
2-Methylbuta-1,3-diene (in cyclohexane)	3.0	5.0
(in ethanol)	4.2	5.9
(in acetonitrile)	5.7	8.3
2,3-Dimethylbuta-1,3-diene	3.9	7.2
4.0	5.7	
1-Methylbuta-1,3-diene	0.35	0.65
1,4-Dimethylbuta-1,3-diene	2.4	4.1
1,1,4,4-Tetramethylbuta-1,3-diene	1.4	2.4
Cyclohexa-1,4-diene ^b	0.04	0.03

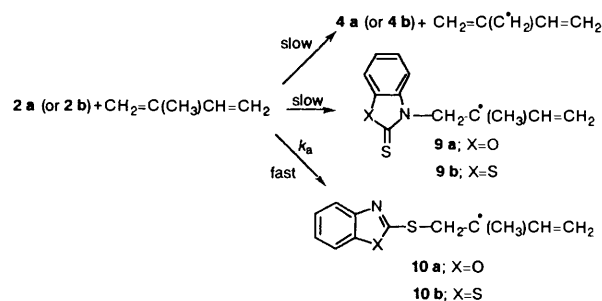
^a Each value may contain an experimental error of $\pm 5\%$. ^b In the rate constant, H-abstraction and addition are included.

slightly accelerated. The rate constants are less than $ca. 4 \times 10^6$ dm 3 mol $^{-1}$ s $^{-1}$, which are $ca. 1/100$ of those for conjugated dienes such as 2-methylbuta-1,3-diene, indicating that the hydrogen abstraction abilities of **2a** and **2b** are far less than the addition abilities to dienes. The low reactivity of cyclohexa-1,4-diene also shows that the addition ability of **2a** and **2b** to the non-conjugative double bond is quite low (Scheme 7).



Scheme 7

On the other hand, high reactivity towards 2-methylbuta-1,3-diene may be due to the high addition reactivities of **2a** and **2b**, not to the hydrogen abstraction reaction from the methyl group, although carbon-centred radicals [$\text{CH}_2=\text{C}(\text{C}^\bullet\text{H}_2)\text{-CH}=\text{CH}_2$, **9** and **10** in Scheme 8] in the product side are



Scheme 8

resonance-stabilized allyl-type radicals. The reactions forming the N–C bond with conjugated dienes (**9**) were excluded, because of the lack of the characteristic thione absorption bands in the product. Thus, the formation of an S–C bond like **10** is most probable.

For most of the dienes, the reactivities of **2a** are quite similar to those of **2b**; **2b** is slightly more reactive than **2a** by a factor of $ca. 1.7$. The trend of reactivities of **2a** towards the dienes is

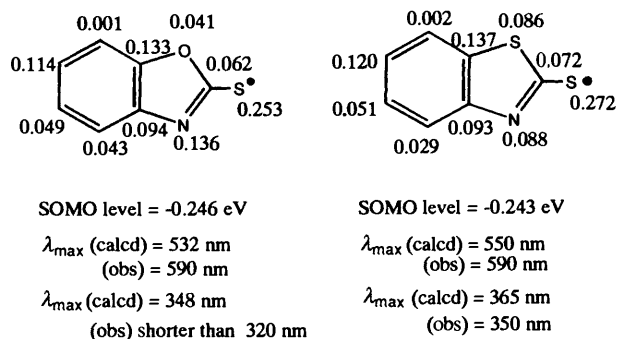


Fig. 9 SOMO energy and the unpaired π -electron density of SOMO of the radicals. The calculated λ_{\max} are also cited with observed values.

similar to that of **2b**. The central two methyl groups of 2,3-dimethylbuta-1,3-diene do not have a considerable effect on the k_a values compared with the mono-substituted methyl group of 2-methylbuta-1,3-diene, suggesting that the addition reaction does not take place at the central carbons of the butadiene moiety.²⁰ The terminal mono-methyl substitution of 1-methylbuta-1,3-diene suppresses the reaction rate compared with 2-methylbuta-1,3-diene, indicating that addition reaction occurs predominantly at the terminal double bond producing the resonance-stable allyl-type radicals.²¹ Dimethyl substitution and tetra-methyl substitution at terminal carbons do not suppress the reactivity as expected from the mono-substitution 1-methylbuta-1,3-diene; this may be attributed to the ability of the methyl group.

In Table 2, the k_a values for the reaction of **2a** and **2b** with 2-methylbuta-1,3-diene in ethanol are greater than those in the other solvents, suggesting some effects of hydrogen bonding between the radicals **2a** (or **2b**) and ethanol. Probably, the N atom of **2a** and **2b** is weakly bound to the H-O of ethanol, which may increase the unpaired electron density at the S atom, thus decreasing the contribution of the N centred radical of **2a** and **2b**.

From the spectroscopic and kinetic data obtained in this study, it is presumed that the unpaired electrons localize mainly on S atoms for the radicals (**2a** and **2b**) produced from **1a** and **1b**. In order to confirm the electronic structures of the ground-state radicals **2a** and **2b**, we investigated the characters of MOs of the radicals using *ab initio* MO calculations. The density functional theory (DFT) treatments have a significant advantage in open-shell calculation of radical species, since the results have far less spin contamination of the wave function than traditional *ab initio* unrestricted Hartree-Fock (UHF) calculations.^{22,23} Hence we employed the DFT method here for the ground-state calculations.

Some results are shown in Fig. 9. Present calculations give persuasive evidence for the experimental results. The unpaired electron of SOMO is mainly localized on the S atom at the 2-position in both radicals, although the SOMOs have π -character which spreads over the p_z -orbitals on the molecular skeleton. Since the p_z function of the S atom has diffuse spatial extent, it can readily overlap with other π -orbitals of the substrates such as dienes. Thus, this provides a reason for the high addition reactivity of radicals **2** to conjugated dienes. The calculated unpaired electron density on the S atom of **2b** is slightly higher than that of **2a**. The observed higher reactivity of **2b** than that of **2a** is thus reasonably interpreted by higher localization of the unpaired electron on the S atom of radical **2b**. The unpaired electron density on the N atom of **2a** is considerably high compared with other atoms within the radical and with that on the N atom of **2b**. This may be related to the appearance of the extra absorption band near 450 nm by the laser flash photolysis of **1a**.

The energy level of the SOMO of **2a** is similar to that of **2b**, suggesting a similarity in the electrophilicity of the

attacking radicals. The effect of spatial overlap of the frontier orbitals plays an important role to account for the difference between the reactivities of **2a** and **2b**.

The transition energies of the radicals were calculated by both *ab initio* and MNDO methods. The same behaviour of the unpaired electron density was found by the MNDO method as was obtained by the *ab initio* method. The transition energies calculated by the MNDO method are listed in Fig. 9, which reproduce the observed transition energies better than those of the *ab initio* method.

Experimental

Materials

Commercially available bis(1,3-benzoxazol-2-yl) disulfide (**1a**), bis(1,3-benzothiazol-2-yl) disulfide (**1b**) and bis(*p*-chlorophenyl) disulfide (**5**) and dienes were used after recrystallization. We prepared **6a** and **6b** by the photolysis of a 1 : 1 mixture of **1a** (0.02 mol dm⁻³) or **1b** (0.02 mol dm⁻³) and **5** (0.02 mol dm⁻³) in benzene solution (degassed with N₂) at room temperature for 1 h with the steady-light longer than 270 nm of Xe-Hg lamp. Disulfides **6a** and **6b** were obtained in an almost equimolar mixture with **1** and **5**. Disulfide **6a** (or **6b**) was separated by TLC (Merck; Kiesegel 60F and benzene as an eluent) and recrystallization from ethanol.

6a: 27% yield (expected yield = 33%), solid; UV; λ_{\max} = 246 and 208 nm. Mp = 89 °C, Anal. Calc. for C₁₃H₈NOS₂Cl: C, 53.15; H, 2.73; N, 4.77; S, 21.71. Found: C, 53.35; H, 3.2; N, 4.35.

6b: 28% yield (expected yield = 33%), solid; UV; λ_{\max} = 270 nm and 220 nm. Mp = 106 °C, Anal. Calc. for C₁₃H₈NS₃Cl: C, 50.40; H, 2.58; N, 4.52; S, 31.02; Cl, 11.47. Found: C, 50.3; H, 2.7; N, 5.85.

Apparatus

Laser flash photolysis apparatus was a standard design with an Nd:YAG laser of 6 ns duration. Solution was photolysed with FHG light (266 nm).²⁴⁻²⁵ The time profiles were followed by a photomultiplier system in the visible region. Transient spectra were recorded with a multi-channel photodiode system. The laser photolysis was performed for the solution in a rectangular quartz cell with 10 mm optical path. The monitoring light was selected with the band-path filters. All the measurements were carried out at 23 °C.

MO calculations

All ground-state calculations were carried out using the GAUSSIAN92 series of *ab initio* MO programs which incorporates the density function theory (DFT) methods (GAUSSIAN92/DFT).²⁶ Geometry optimization and population analyses were carried out with a hybrid method (Becke3LYP),²⁷ which includes a mixture of Hartree-Fock exchange with DFT exchange correlations.

Transition energies were obtained by a single excitation CI. First, the geometry of the radical was optimized using 3-21G* basis sets which are medium sized in these type of calculations to save computational costs. Consequent calculations were carried out using the polarized bases 6-311G** which have d-functions on heavy atoms to include the effect of the diffuse nature of p-orbitals of the S atom into account.

The electron densities were also calculated by the MNDO method. The transition energies were obtained by single excitation CI after semi-empirical MNDO unrestricted Hartree-Fock MO calculations using MOPAC program package.²⁸

References

- Ed. F. F. Eirich, *Science and Technology of Rubber*, Academic Press, New York, 1978.

- 2 S. Tamura and K. Murakami, *Polymer*, 1980, **21**, 1398.
- 3 T. Sato, M. Abe and T. Otsu, *Makromol. Chem.*, 1977, **178**, 1951.
- 4 T. Sato, M. Abe and T. Otsu, *Makromol. Chem.*, 1979, **180**, 1165.
- 5 O. Ito, K. Nogami and M. Matsuda, *J. Phys. Chem.*, 1981, **85**, 1365.
- 6 O. Ito and M. Matsuda, *Chemical Kinetics of Organic Small Molecules*, ed. Z. B. Alfassi, CRC Press, Boca Raton, 1989, vol. 3, ch. 15.
- 7 O. Ito and M. Matsuda, *Prog. Polymer Sci.*, 1992, **17**, 827.
- 8 P. Beak, *Acc. Chem. Res.*, 1980, **45**, 1347.
- 9 F. C. Thyron, *J. Phys. Chem.*, 1973, **77**, 1478.
- 10 M. Nakamura, O. Ito and M. Matsuda, *J. Am. Chem. Soc.*, 1980, **102**, 698.
- 11 O. Ito and M. Matsuda, *J. Am. Chem. Soc.*, 1979, **101**, 1815.
- 12 T. J. Burkey and D. Griller, *J. Am. Chem. Soc.*, 1985, **107**, 246.
- 13 O. Ito, S. Tamura, K. Murakami and M. Matsuda, *J. Polymer Sci.*, 1988, **26**, 1429.
- 14 H. Shizuka, K. Kubota, T. Morita, *Mol. Photochem.*, 1972, **3**, 335.
- 15 K. U. Ingold, in *Free Radicals*, ed. J. K. Koch, Wiley, New York, 1973, p. 37.
- 16 C. Chatgililoglu and K.-D. Asmus, *Sulfur-Centered Reactive Intermediates in Chemistry and Biology*, NATO ASI Series A: Life and Science Vol. 197, Plenum Press, New York, 1990, pp. 327–340.
- 17 M. M. Alam, A. Watanabe and O. Ito, *J. Org. Chem.*, 1995, **60**, 3440.
- 18 H. Paul, R. D. Small, Jr., and J. C. Scaiano, *J. Am. Chem. Soc.*, 1978, **100**, 4520.
- 19 M. Newcomb and S. U. Park, *J. Am. Chem. Soc.*, 1986, **108**, 4132.
- 20 A. A. Oswald, K. Gresbaum, W. A. Thaler and B. E. Hudson, *J. Am. Chem. Soc.*, 1962, **84**, 3897.
- 21 O. Ito, S. Tamura, K. Murakami and M. Matsuda, *J. Org. Chem.*, 1988, **53**, 4758.
- 22 M. J. Shephard and M. N. Paddon-Row, *J. Phys. Chem.*, 1995, **99**, 3101.
- 23 J. Baker, A. Schneider and J. Andzelm, *Chem. Phys. Lett.*, 1993, **216**, 380.
- 24 A. Watanabe and O. Ito, *J. Chem. Soc., Chem. Commun.*, 1994, 1285.
- 25 A. Watanabe and O. Ito, *J. Phys. Chem.*, 1994, **98**, 7736.
- 26 M. J. Frisch, G. W. Trucks, H. B. Schlegel, P. M. W. Gill, B. G. Johnson, M. W. Wong, J. B. Foresman, M. A. Robb, M. Head-Gordon, E. S. Replogle, R. Gomperts, J. L. Andres, K. Raghavachari, J. S. Binkley, C. Gonzalez, R. L. Martin, D. J. Fox, D. J. Defrees, J. Baker, J. J. P. Stewart and J. A. Pople, *GAUSSIAN92/DFT, Revision G.3*, Gaussian, Inc., Pittsburgh, 1993.
- 27 (a) A. D. Becke, *Phys. Rev. Part B*, 1988, **38**, 3098; (b) C. Lee, W. Yang and R. G. Parr, *Phys. Rev. Part B*, 1988, **37**, 785; (c) S. H. Voski, L. Wilk and M. Nusair, *Can. J. Phys.*, 1980, **58**, 1200.
- 28 J. J. Stewart, *QCPE Bull.* 1989, **9**, 10.

Paper 5/00286I

Received 17th January 1995

Accepted 13th October 1995